

Syracuse University

**SURFACE**

---

Physics

College of Arts and Sciences

---

2008

## Energy-dependent Ps-He momentum-transfer cross section at low energies

Joseph Paulsen  
*Syracuse University*

Follow this and additional works at: <https://surface.syr.edu/phy>



Part of the [Physics Commons](#)

---

### Recommended Citation

Paulsen, Joseph, "Energy-dependent Ps-He momentum-transfer cross section at low energies" (2008).  
*Physics*. 519.  
<https://surface.syr.edu/phy/519>

This Article is brought to you for free and open access by the College of Arts and Sciences at SURFACE. It has been accepted for inclusion in Physics by an authorized administrator of SURFACE. For more information, please contact [surface@syr.edu](mailto:surface@syr.edu).

## Energy-dependent Ps-He momentum-transfer cross section at low energies

J. J. Engbrecht, M. J. Erickson, C. P. Johnson, A. J. Kolan, A. E. Legard, S. P. Lund, M. J. Nyflot, and J. D. Paulsen  
*Saint Olaf College, Northfield, Minnesota 55057, USA*  
 (Received 18 June 2007; published 17 January 2008)

Positronium (Ps)-He scattering presents one of the few opportunities for both theory and experiment to tackle the fundamental interactions of Ps with ordinary matter. Below the dissociation energy of 6.8 eV, experimental and theoretical work has struggled to find agreement on the strength of this interaction as measured by the momentum-transfer cross section ( $\sigma_m$ ). Here, we present work utilizing the Doppler broadening technique with an age-momentum correlation apparatus. This work demonstrates a strong energy dependence for this cross section at energies below 1 eV and is consistent with previous experimental results.

DOI: [10.1103/PhysRevA.77.012711](https://doi.org/10.1103/PhysRevA.77.012711)

PACS number(s): 36.10.Dr, 34.50.-s, 78.70.Bj

Positronium-He scattering provides one of the only systems in which Ps interactions with ordinary matter can be explored both theoretically and experimentally. At low energies, the correlation effects between positrons ( $e^+$ ) and electrons are strongest, making this a particularly interesting region. Unfortunately, achieving consistency between and within experimental and theoretical results has been difficult below the dissociation threshold of Ps (6.8 eV). This work aims to rectify the experimental inconsistency by exploring the momentum-transfer cross section ( $\sigma_m$ ) with a broader energy range and higher precision.  $\sigma_m$  differs from the total cross section by weighting the differential cross section by a factor of  $[1 - \cos(\theta)]$ . At zero energy where scattering is completely  $s$  wave,  $\sigma_m$  is equal to the total cross section.

Experimentally, Ps beams have not provided results below 10 eV due to technical challenges [1]. Ps-He scattering cross sections below this energy range were made by Canter *et al.* [2] using lifetime measurements of Ps trapped in a bubble state in liquid He. This work yielded a total scattering cross section of  $7.1 \pm 0.5 \text{ \AA}^2$ . Later work identified possible systematic errors in the technique used in Canter *et al.*, but an improved experiment by Rytola *et al.* [3] seemed to confirm the end result with a value of  $7.5 \pm 0.4 \text{ \AA}^2$ . These values are essentially measurements of the cross section at zero energy as the Ps was at cryogenic thermal energies of  $\sim 1$  meV.

More recently, observing the thermalization process of Ps in a gas environment has been used.  $e^+$ 's introduced into a gas environment will form ground state Ps with energies of a few eV [4]. The Ps will then thermalize through elastic collisions with He. Because these collisions determine the thermalization rate, measurements of this rate yield information on  $\sigma_m$ . These experiments take advantage of the unique properties of Ps. When Ps is at rest and decays into two  $\gamma$  rays, conservation of momentum and energy determine that  $\gamma$  rays of equal energy (511 keV) will be produced at  $180^\circ$ . Deviations in both the energies and the relative angle of the  $\gamma$  rays occur when the Ps is in motion. Observations of these deviations therefore measure the velocity of the Ps.

Deviations in the  $180^\circ$  formed by the annihilation  $\gamma$  rays were studied with angular correlation of annihilation radiation (ACAR) by Coleman *et al.* [5] and Nagashima *et al.* [6] to measure  $\sigma_m$ . Coleman *et al.* reported a  $\sigma_m$  of  $7.9 - 0.4E \text{ \AA}^2$ , where  $E$  is the Ps energy in eV. Due to systematic issues and limited data, the authors did not report an

error estimate. Nagashima *et al.* also used ACAR to measure a  $\sigma_m$  of  $11 \pm 3 \text{ \AA}^2$ . This work introduced the use of variable magnetic fields to change the Ps lifetime and silica aerogel to confine the gas and Ps to a small volume.

Ps thermalization was also observed using Doppler broadening (DB) to look at the energy deviation of the annihilation  $\gamma$  rays in Skalsey *et al.* [7]. The DB technique has lower energy resolution than does ACAR, but a much higher data rate. This work reported a low  $\sigma_m$  of  $2.8 \pm 3 \text{ \AA}^2$ , though the energy of the Ps observed was much higher than the other experimental methods.

The consistency of the systematically different experiments from Refs. [2,3,5,6] produces confidence in their results. This has been enhanced in recent years by theoretical results [8–12] that produced zero energy cross sections similar to the lower energy experiments while deviating from the DB work. There are two likely explanations for the DB result. First, the DB experiment contains an error or DB is in some way inherently unsuitable for these studies. Second, the Ps-He  $\sigma_m$  is strongly energy dependent. No evidence has been presented to support the first possibility. Likewise, for various reasons (lack of data [5,7], inherently limited energy range [2,3], or competing systematics [6]) no experiment has been able to demonstrate a  $\sigma_m$  energy dependence large enough to resolve the discrepancy.

This situation made it clear that further experimental work was necessary. Only the DB technique presented an opportunity for significant improvements and was therefore chosen for our experiment. We improve detector stability and resolution as well as systematic tests and data rates. This is accomplished with an age-momentum correlation (AMOC) apparatus (Fig. 1) that records the lifetime and DB of each Ps event [13,14]. A  $^{22}\text{Na}$  source emits  $e^+$ 's that pass through a thin (0.15 mm) plastic scintillator and enter the gas chamber, marking the time of  $e^+$  emission. A magnetic field of  $\sim 0.25$  T confines the  $e^+$ 's along a helical path until they form Ps.

To study Ps thermalization, two conditions need to be met: the Ps must live 10's of ns and must undergo two photon annihilation. Ps forms two ground states, spin-0 parapositronium ( $p$ -Ps) and spin-1 orthopositronium ( $o$ -Ps).  $p$ -Ps undergoes two photon annihilation but has a lifetime of 125 ps.  $o$ -Ps has a lifetime of 142 ns, but produces three photons in its annihilation. Thus a magnetic field is applied

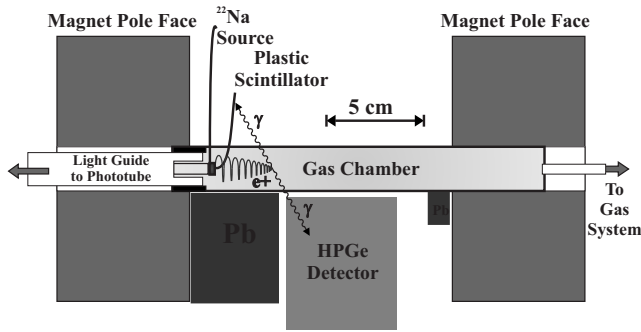


FIG. 1. Apparatus schematic.

that mixes the  $m_s=0$   $o$ -Ps state with the single  $p$ -Ps state. In our  $B$  field, the created mixed  $o$ -Ps state lives  $\sim 61$  ns and decays via two  $\gamma$  rays  $\sim 55\%$  of the time [15]. This state of Ps will thermalize until it annihilates. The annihilation radiation is detected by a high-purity germanium detector (HPGe) that determines the time and energy of the annihilation  $\gamma$  rays for use in the DB analysis. The Ps formation time is short ( $\ll 1$  ns) relative to its lifetime, and thus we have measured the Ps lifetime.

The detector signals are processed by the data acquisition system outlined in Ref. [13,14]. This system digitizes the timing and energy signals of an individual Ps signal and sends them to a coincidence circuit. This circuit, along with LabVIEW software, sorts the data into three spectra: separate time and energy spectra regardless of correlation between the two, and a two-dimensional (2D) time and energy spectra for coincident data. The location of a 662 keV energy peak from a  $^{137}\text{Cs}$  source is tracked and the amplification of the energy signal is adjusted to prevent peak drift in the energy spectrum.

Our data was saved in 4 h increments during week long data acquisition runs using pressures of 4, 6, 8, 12, and 16 psi at a temperature of 305 K. Total data acquisition time was 2750 h. In Fig. 2(a), the raw data for 16 psi is shown. The nearly flat background is subtracted on the high and low energy sides of the 511 keV peak as shown in Fig. 2(b) using a sloping step function convolved with a Gaussian of appropriate width.

The 511 keV peak remains, including signals from thermalizing  $o$ -Ps and a number of background signals. At  $t=0$  there are events from both  $p$ -Ps that has formed and  $e^+$ 's that have collided with the chamber wall. With a timing resolution of 5 ns full width at half maximum (FWHM), only data 20 ns after  $t=0$  can be usefully analyzed without these events interfering with analysis.

At later times, the background comes from a variety of sources including slow  $e^+$ 's that have lost the energy needed to form Ps,  $e^+$ 's from  $o$ -Ps that annihilate with electrons from a He atom during a collision, and uncorrelated  $e^+$  annihilations. Each of these sources of background derive their DB from the high momentum of electrons bound to atoms in the gas or gas chamber wall and are therefore broader than the thermalizing Ps signal [6,7]. At times 400–700 ns, all magnetically perturbed  $o$ -Ps has decayed. This time window is used to determine the shape of the broad background events. Data in earlier time windows is then corrected by scaling this

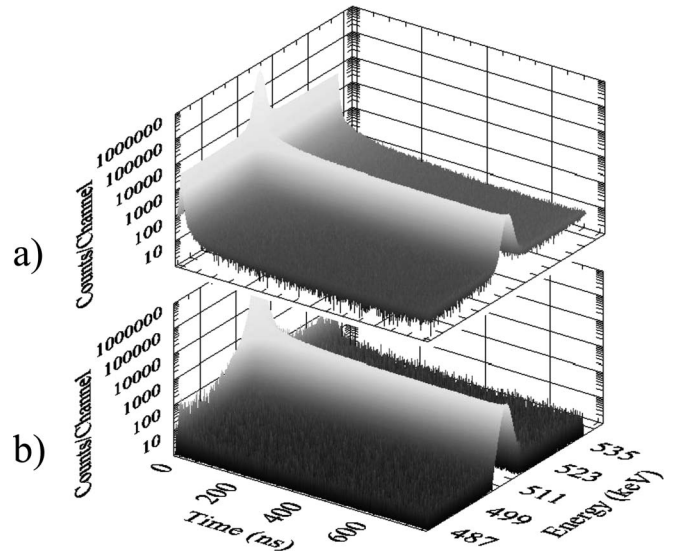


FIG. 2. 2D time and energy spectrum. (a) Data for 16 psi of the 511 keV peak as a function of time. (b) Data with the low and high energy backgrounds removed.

broad spectrum for subtraction. Figure 3 shows an example of this process. In order to make the background as flat as possible, we subtract an additional very wide (8.9 keV FWHM) Gaussian component. The origin of this component is not entirely clear, though it may represent a deviation in the shape of the background components in different time windows. This is not surprising as the relative sizes of the contributions to this background are certainly a function of time and slight changes should be expected. In order to ensure that our results are not sensitive to the particular shape of this small component, we vary its FWHM from

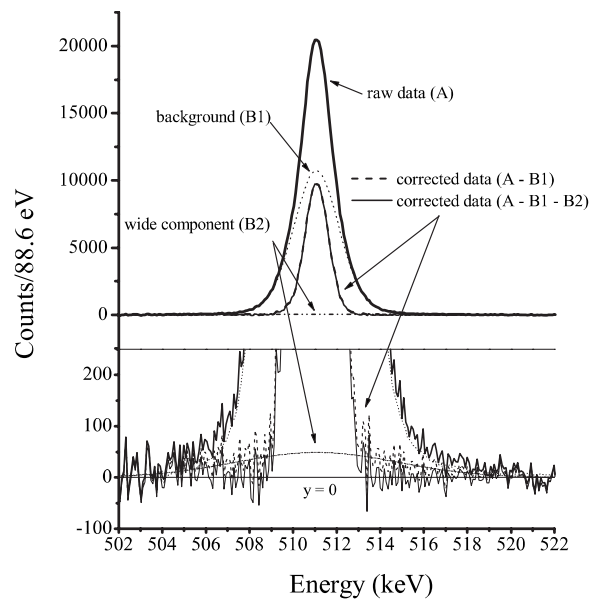


FIG. 3. Data correction—16 psi data from late time (400–700 ns) is summed (B1) and scaled to remove this component from the data at an earlier time of 25–30 ns(A). An additional, very small wide component is also removed (B2) to yield the flattest background possible as shown in (A-B1-B2).

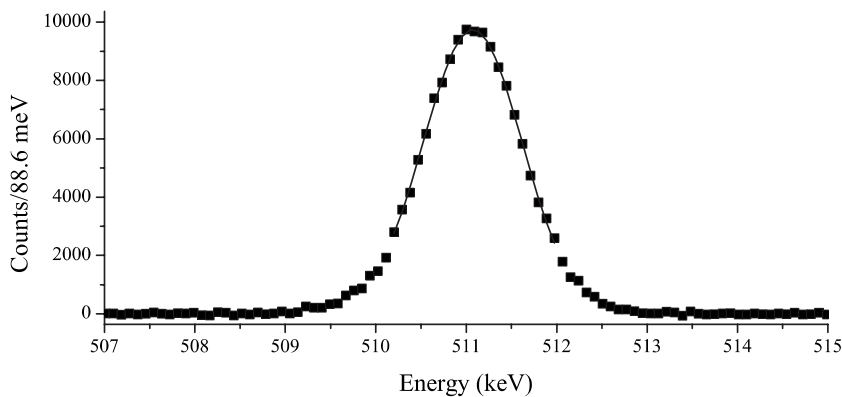


FIG. 4. DB fit—A fit of 16 psi data at 25–30 ns using a single gaussian convolved with the detector resolution.

7.4 keV to 14.8 keV and do not see a significant change in our results.

The remaining data is fit to find the FWHM of the DB. The HPGe detector resolution is determined by fitting the  $^{137}\text{Cs}$  662 keV peak to two Gaussians, one of which is convolved with two exponential tails. This resolution is energy dependent and thus must be scaled before it is applied to the 511 keV peak. This scaling factor is determined by measuring the FWHM from  $^{137}\text{Cs}$  and  $^{133}\text{Ba}$  peaks at 662, 276.4, 302.9, 356.0, and 383.9 keV and interpolating. This process yields a FWHM of 1.41 keV at 511 keV. The scaled detector resolution is then convolved with a single Gaussian and fit to the thermalizing  $o$ -Ps signal. Data is analyzed in 5 ns time windows from 20 to 60 ns after  $t=0$ . The FWHM,  $W$ , of the DB is then converted to an average energy,  $E$ , of the  $o$ -Ps using Eq. (1) [7] which assumes a Maxwell-Boltzmann distribution of Ps energy. An example of this fit is shown in Fig. 4,

$$E(\text{eV}) = [1.0228W(\text{keV})]^2. \quad (1)$$

The statistical uncertainty in these Ps energy values is affected by many parts of the data analysis procedure and is difficult to assess through standard statistical means. Therefore, a bootstrap process is employed [16]. The original data is randomized using the Poisson statistics determined by the data itself. This randomized data is subjected to the same analysis procedure as the original data. The process is repeated 10 times and a standard deviation of each Ps energy fit is found.

These energies are then plotted vs pressure  $\times$  time to produce Fig. 5 and fit with the result of Ref. [6,17],

$$\frac{d}{dt}E_{av}(t) = -\sqrt{2m_{Ps}E_{av}(t)}[E_{av}(t) - E_{th}] \left( \frac{8}{3} \sqrt{\frac{2}{3\pi}} \frac{2\sigma_m(E)n}{M} \right). \quad (2)$$

Here  $E_{av}$  is the average energy of the Ps,  $t$  is time,  $n$  is the density of He atoms,  $E_{th}$  is the thermal energy of the gas, and  $M$  and  $m_{Ps}$  are the masses of He and Ps, respectively. This differs from the equations used in Skalsey *et al.* [7] by a factor of  $\frac{8\sqrt{2}}{3\sqrt{3\pi}} \approx 1.228$ , which used the results of Ref. [17]. The more complete treatment of thermalization theory in Ref. [6] yields a result that is different by this factor. We use the result from Ref. [6] here and suggest that the Skalsey *et al.* result be lowered by this factor to  $2.3 \pm 0.7 \text{ \AA}^2$ .

Important systematic checks are visible in Fig. 5. No systematic variation is apparent between the various gas pressures used. Since each gas pressure has different signal to background ratios for a given value of pressure  $\times$  time, this is a strong test of our analysis method. Another important systematic test is our asymptotic approach to thermal energies where we simultaneously have the lowest data rates, the lowest signal to background ratio, and the least amount of DB. None of the previous experiments achieved these or similar systematic checks for various technical reasons.

The result of fitting Eq. (2) to our data with an energy independent  $\sigma_m$  is  $2.05 \pm 0.11 \text{ \AA}^2$ . The reduced  $\chi^2$  is 1.38. The error is reduced by a factor of 7 from the previous DB result of Skalsey *et al.* [7]. The elevated  $\chi^2$  indicates that an energy independent  $\sigma_m$  is not sufficient to fit the data. We therefore implement energy-dependent cross sections into Eq. (2) including a linear, a quadratic, and a cubic dependence. The linear dependence produces a  $\sigma_m$  that decreases slightly with increasing energy, but  $\chi^2$  stays at 1.38. A quadratic dependence for  $\sigma_m$  dramatically reduces  $\chi^2$  to 0.95. The best fit parameters for  $\sigma_m$  with this fit are  $\sigma_m = 4.9 - 11.1E + 8.5E^2$ . Here  $\sigma_m$  has units of  $\text{\AA}^2$  and  $E$  has units of eV. This function has a minimum at  $\sim 0.6$  eV. The rising on the high-energy side of this minimum is highly dependent on the single data point at 1.8 eV. Deletion of this point re-

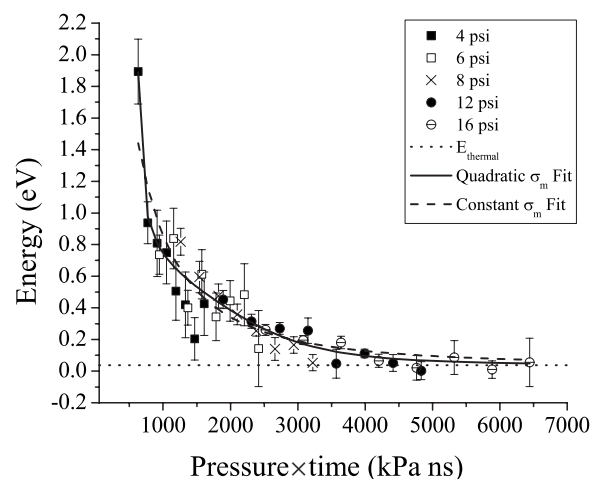


FIG. 5. Thermalization results—best fits for  $\sigma_m$  held constant and allowed a quadratic dependence shown with all of the DB results.

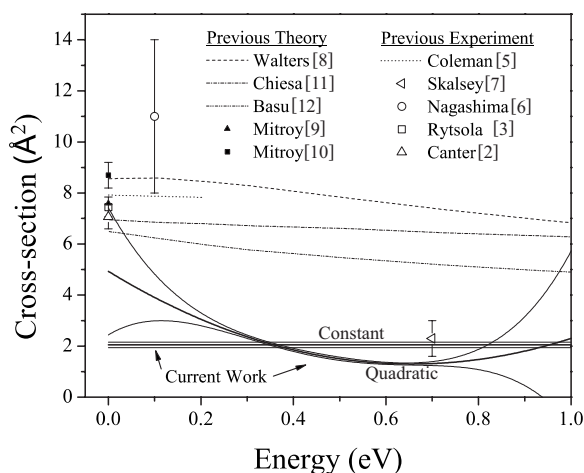


FIG. 6. Summary of cross section results for Ps-He scattering. All results are for  $\sigma_m$  except Chiesa *et al.*, which is a total cross section. Results from this work are represented by a bold line to indicate the best fit of the data and thin lines to represent estimates of the error for the given model.

moves the statistical significance of the rising  $\sigma_m$  at increasing energies. On the low-energy side, the increasing  $\sigma_m$  is much more robust. Allowing  $\sigma_m$  to have a cubic dependence produces no further reduction in  $\chi^2$ . The results of the constant and quadratic (without the 1.8 eV point) fits are shown in Figs. 5 and 6. The errors shown are determined using the covariance matrix produced during fitting and represent estimates of 1 standard deviation from the best fit.

The striking feature of Fig. 6 is the indication that all current and previous experiments may be consistent. The quadratic  $\sigma_m$  overlaps with Skalsey *et al.* and rises at lower energies to nearly reach (within error) the experiments of Canter *et al.* [2] and Rytsola *et al.* [3], which used lifetime measurements of Ps in liquid He. The ACAR results of Coleman *et al.* [5] and Nagashima *et al.* [6] do seem a bit high compared to the quadratic  $\sigma_m$ . Given the lack of an uncertainty estimate by Coleman *et al.* and the large uncertainty reported by Nagashima *et al.* we do not consider these experiments to be in serious disagreement with the results presented here. Experimental evidence, therefore, paints a consistent picture of a highly energy-dependent cross section that is in clear disagreement with theoretical calculations. We suggest that more theoretical work will be necessary to resolve this.

In the future, we plan to study other noble gases and diatomic molecules for a similar energy dependence. This work will also explore the possibility of using gas mixtures to obtain improved data at low energies. We are also pursuing ideas for the generation of Ps beams at energies below 1 eV.

The authors would like to thank J. Walters, M. Bromley, Y. Nagashima, and D. Gidley for helpful discussion related to this work and B. N. Costanzi, D. E. Endean, D. J. Green, and G. J. Williams for help in manuscript preparation. Support for this work was provided by Research Corporation, NSF Grant No. 0555631, the Saint Olaf Physics Department, and HHMI.

- 
- [1] A. J. Garner, A. Özen, and G. Laricchia, *J. Phys. B* **33**, 1149 (2000).
  - [2] K. Canter, J. McNutt, and L. Roellig, *Phys. Rev. A* **12**, 375 (1975).
  - [3] K. Rytsola, J. Vettenranta, and P. Hautajarvi, *J. Phys. B* **17**, 3359 (1984).
  - [4] A. Öre, *Naturvidenskap Rikke No. 9* (University of Bergen, Arbok, 1949).
  - [5] P. Coleman, S. Rayner, F. Jacobsen, M. Charlton, and R. West, *J. Phys. B* **27**, 981 (1994).
  - [6] Y. Nagashima, T. Hyodo, K. Fujiwara, and A. Ichimura, *J. Phys. B* **31**, 329 (1998).
  - [7] M. Skalsey, J. J. Engbrecht, C. M. Nakamura, R. S. Vallery, and D. W. Gidley, *Phys. Rev. A* **67**, 022504 (2003).
  - [8] H. Walters, A. Yu, and S. Gilmore, *Nucl. Instrum. Methods Phys. Res. B* **221**, 149 (2004).
  - [9] J. Mitroy, *Phys. Rev. A* **72**, 062707 (2005).
  - [10] J. Mitroy and I. A. Ivanov, *Phys. Rev. A* **65**, 012509 (2001).
  - [11] S. Chiesa, M. Mella, and G. Morosi, *Phys. Rev. A* **66**, 042502 (2002).
  - [12] A. Basu, P. K. Sinha, and A. S. Ghosh, *Phys. Rev. A* **63**, 052503 (2001).
  - [13] J. J. Engbrecht, *Nucl. Instrum. Methods Phys. Res. B* **119**, 221 (2004).
  - [14] J. J. Engbrecht, A. Kolan, C. Johnson, A. Legard, and S. Lund, *Phys. Status Solidi C* **4**, 3443 (2007).
  - [15] A. Rich, *Phys. Rev. A* **23**, 2747 (1981).
  - [16] W. Press, S. Teukolsky, W. Vetterling, and B. Flannery, *Numerical Recipes in C++*, 2nd ed. (Cambridge University Press, New York, 2002).
  - [17] W. C. Sauder, *J. Res. Natl. Bur. Stand., Sect. A* **72**, 91 (1968).